Consequences of Progressive Full-Thickness Focal Chondral Defects Involving the Medial and Lateral Femoral Condyles After Meniscectomy

A Biomechanical Study Using a Goat Model

Jason L. Koh,*† MD, Kevin C. Jacob,‡ BS, Rohan Kulkarni,‡ MS, Zachary Vasilion,† BS, and Farid M.L. Amirouche,†‡ PhD

Investigation performed at Department of Orthopaedic Surgery, Orthopaedic and Spine Institute, NorthShore University HealthSystem, Evanston, Illinois, USA

Background: Full-thickness chondral defects alter tibiofemoral joint homeostasis and, if left untreated, have the potential to progress to osteoarthritis.

Purpose: To assess the effects of isolated and dual full-thickness chondral defect size and location on the biomechanical properties of the lateral femoral condyle (LFC) and medial femoral condyle (MFC) during dynamic knee flexion in goat knees without menisci.

Methods: In 12 goat knees, we created progressively increasing full-thickness circular chondral defects (3-, 5-, and 7.5-mm diameter) in the weightbearing contact area of flexion and extension in the MFC, the LFC, or both. Each knee was fixed into a custom steel frame and attached to a motor with sensors inserted intra-articularly. For each testing condition, the knee was loaded to 100 N and underwent a dynamic range of motion between 90° of flexion and 30° of extension. The following parameters were collected: contact area, contact pressure, contact force, peak area, and peak pressure.

Study Design: Controlled laboratory study.

Results: The peak pressure at the defect rim of the MFC at full extension increased by 51.51% from no defect (1.887 MPa) to a 7.5-mm defect (2.859 MPa) ($P < .001$), and the peak pressure at the defect rim of the LFC at full extension increased by 139.14% from no defect (1.704 MPa) to a 7.5-mm defect (4.075 MPa) ($P < .001$). The peak pressures for LFC defects at all 3 diameters were significantly greater when compared with dual defects consisting of increasing LFC defect diameter and constant MFC defect diameter ($P < .001$ for all).

Conclusion: Extremely large increases in peak pressure were seen at the rim of articular cartilage defects when evaluated under dynamic loading conditions. Isolated LFC defects experienced a greater increase in defect rim stress concentrations when compared with isolated MFC defects for equivalent increases in defect size. Defect size played a significant role independent of location for peak pressures on the MFC and LFC.

Clinical Relevance: Significant rim-loading effects increase with defect size under dynamic loading and may result in increasingly rapid progression of articular cartilage lesions. Within the context of this goat model, findings suggest that lateral compartment chondral lesions are more likely to progress than medial compartment lesions of equivalent size.

Keywords: knee; articular cartilage; meniscectomy; chondral defect

Focal, full-thickness chondral defects within the human knee have the potential to progress to osteoarthritis over time.[8,10,13,31] Progression to osteoarthritis is multifactorial and has been shown to involve subchondral bone changes, a marked rise in defect rim stress concentration, and biomechanical overload of opposing articular surfaces, which lead to modification of tibiofemoral joint homeostasis and subsequent condylar cartilage degeneration.[3,6,8,13,24,31,33]

The Orthopaedic Journal of Sports Medicine, 10(3), 23259671221078598
DOI: 10.1177/23259671221078598

Cartilage degeneration of the knee frequently follows meniscectomy, primarily resulting from elevated contact and stresses as well as dramatically altered compartmental load transmission.[26] Although the biomechanical consequences of lateral and medial meniscectomies involve elevated stress concentration gradients and decreased contact areas, clinical results after lateral meniscectomies have reported poorer outcomes.[26,32] Alford et al[2] noted that there was a relatively higher risk of tibiofemoral articular degeneration and a greater propensity for rapid articular cartilage deterioration in patients after a lateral meniscectomy when compared with a medial meniscectomy. Their finding coincided with the work put forth by Englund and Lohmander,[7] who reported radiological osteoarthritis in 58% of lateral meniscectomies vs 45% of medial meniscectomies at 15 to 22 years of follow-up.

Current clinical treatment options for cartilage defects are largely determined by a threshold defect size of 2 cm^2. This predetermined size threshold has been challenged, and the utilization of other defect-specific factors has been raised to supplement current defect treatment algorithms.[1,13] To better understand the biomechanical basis for increased cartilage degeneration after lateral vs medial meniscectomy, the interaction of defect size and condyle location on defect rim pressures must be explored.

For the current study, we used goat knees without menisci to evaluate the effects of isolated and dual full-thickness chondral defect size and location on the biomechanical properties of the lateral femoral condyle (LFC) and medial femoral condyle (MFC) at the defect rim. We hypothesized that for equivalent increases in defect diameter, mean peak pressures at the defect rim on the LFC would be significantly greater than on the MFC.

METHODS

Twelve fresh-frozen caprine knees were acquired for this study. A goat model was chosen for this study based on the animal-selection guide proposed by Proffen et al[28] and Moran et al,[22] which indicated that the animal model was suitable for biomechanical simulation of the tibiofemoral joint. Before use, specimens were thawed for 24 hours. Once thawed, skin and subcutaneous adipose tissue were removed. Medial and lateral parapatellar arthrotomies were made, and the extensor mechanism was removed. The long digital extensor and popliteus were removed. Both menisci were removed at their respective horn insertions. Collateral and cruciate ligaments were kept intact. Extraneous soft tissue on the distal femur/proximal tibia was removed. Knees with any visible defects were excluded. Though the removal of both menisci does not represent in vivo loading conditions, it was necessary to ensure accurate and precise defect placement and obtain contact parameters around the defect; this is similar to the approach taken by prior biomechanical studies that analyzed the chondral defect and tibiofemoral contact in cadaveric knees.[3,8,9]

Each knee was positioned at 90° of flexion within a custom-fabricated steel frame, with the femur rigidly fixed within a steel column by screws. Each knee was additionally attached to a motor. As the extensor mechanism had been removed prior, the motor enabled the knee to be moved through its range of motion, allowing for data to be collected. Digital electronic pressure sensors (K-Scan; Tekscan) were placed between articulating surfaces of the femoral condyles. A 2-point calibration was performed, and sensors were recalibrated after each set of trials for a single knee to ensure accuracy and precision. Calibration using load cell measurements from the same trial eliminated trial-to-trial calibration drift. To apply load to our specimens, a hole was drilled through the tibia and parallel to the joint line. A rod was inserted and connected to a pulley system that allowed for incremental load attachments (Figure 1).

A 100-N load was applied orthogonal to the tibial surface at full extension (30°) and flexion (90°), and contact areas were outlined circumferentially on the femoral condyles with a surgical marker. After the intended defect area was specified, specimens were removed from the fixation apparatus to allow for access to articular surfaces. With the use of a mechanical coring punch, full-thickness circular chondral defects of progressively increasing diameter (3, 5, and 7.5 mm) were created at the weightbearing contact area for flexion and extension in the MFC, LFC, or both on each knee (Figure 2).

The upper limit of 7.5 mm for the defect size was chosen as Schinhan et al[31] demonstrated in sheep that a 7-mm defect was the threshold size at which unicompartmental osteoarthritis was induced. Diameter width was controlled with a digital caliper. Four groups consisting of 3 knees in each group were tested, and a baseline reading of each knee before testing was obtained (Table 1).

Loading

For each group, the knee was attached to a motor and fixed within a custom steel frame. The apparatus consisted of a weighted pulley system that enabled approximately equal contact between the medial and lateral condyles under motor-enabled flexion and extension. The loading apparatus did not adjust for rotation/translation, and varus and

*Address correspondence to Jason L. Koh, MD, Department of Orthopaedic Surgery, Orthopaedic and Spine Institute, NorthShore University HealthSystem, 2650 Ridge Ave, Suite 2505, Walgreen Building, Evanston, IL 60201, USA (email: jkoh@northshore.org).
†Department of Orthopaedic Surgery, Orthopaedic and Spine Institute, NorthShore University HealthSystem, Evanston, Illinois, USA.
‡Department of Orthopaedic Surgery, University of Illinois, Chicago, Illinois, USA.
Final revision submitted October 14, 2021; accepted November 30, 2021.
One or more of the authors has declared the following potential conflict of interest or source of funding: J.L.K. has received education payments from Medwest and research support, consulting fees, and royalties from Flexion. AOSSM checks author disclosures against the Open Payments Database (OPD). AOSSM has not conducted an independent investigation on the OPD and disclaims any liability or responsibility relating thereto.
Ethical approval was not sought for the present study.

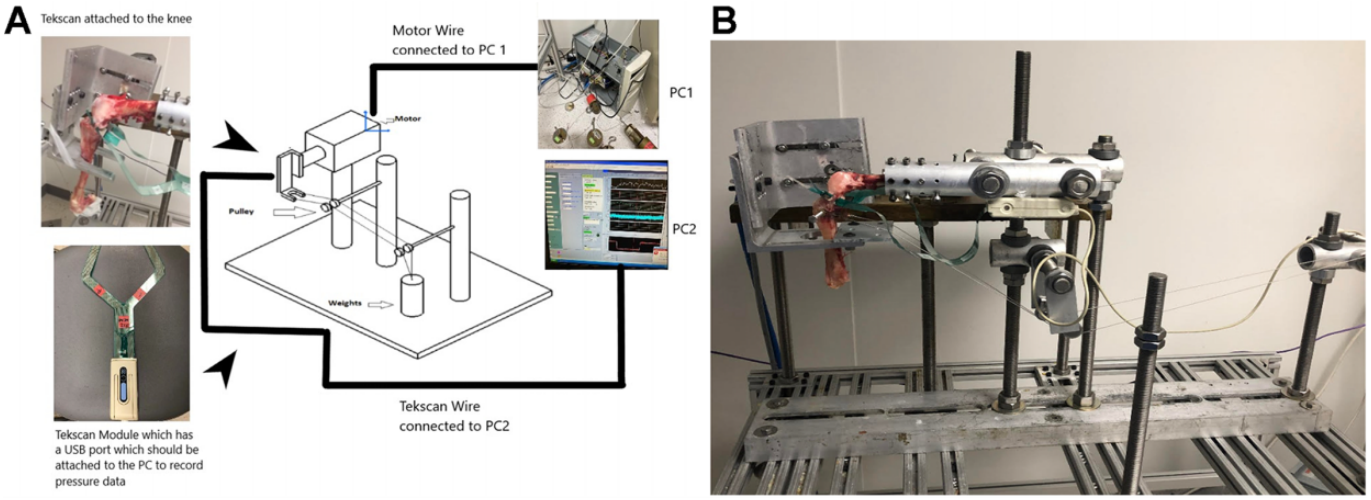

Figure 1. (A) Experimental setup. (B) Femoral fixation apparatus with goat knee positioned at 90° of flexion within a custom steel frame and attached to a pulley system and motor. Tekscan K-Scan sensors were inserted intra-articularly to record pressures around the defect. PC, personal computer.

Figure 2. A 7.50-mm defect on a medial femoral condyle created using a mechanical coring punch.

valgus motion was unconstrained. Tekscan K-Scan sensors were reinserted into the joint. The starting position of the specimen was at 90° of flexion. The knee was loaded to 100 N, and the motor turned on (50 seconds, 5 cycles, 10 s/cycle). The range of motion for the knee was 60° (ie, between 90° of flexion and 30° of extension). The following parameters were collected: contact area, contact pressure, contact force, peak area, peak pressure, and pressure distribution (Figure 3). Given the unequal variances for peak pressures with regard to different defect sizes, a Kruskal-Wallis test was used to evaluate the influence of defect size on defect rim peak pressure. Post hoc pairwise comparisons were obtained with the Dunn-Bonferroni approach.

TABLE 1
Description of Experimental Groups[a]

Group	No.	Condition
1	12	No defect (baseline reading for the knees in each group)
2	3	Increasing defect size on MFC (3 mm, 5 mm, 7.5 mm), no defect on LFC
3	3	Increasing defect size on LFC (3 mm, 5 mm, 7.5 mm), no defect on MFC
4	3	Increasing defect size on MFC (3 mm, 5 mm, 7.5 mm), constant 3-mm defect on LFC
5	3	Increasing defect size on LFC (3 mm, 5 mm, 7.5 mm), constant 3-mm defect on MFC

[a]Knees in all groups underwent loading to 100 N. LFC, lateral femoral condyle; MFC, medial femoral condyle.

RESULTS

In knees with no defect, the peak pressure on the MFC (1.887 MPa) was significantly greater than that on the LFC (1.704 MPa) ($P < .001$) (Figure 4). In the group 2 knees, the peak pressure at the defect rim for the MFC at full extension increased by 51.51% from no defect (1.887 MPa) to a 7.5-mm defect (2.859 MPa) ($P < .001$) and by 25.9% from a 3-mm defect (2.279 MPa) to a 7.5-mm defect (2.869 MPa) ($P < .008$) (Figure 5).

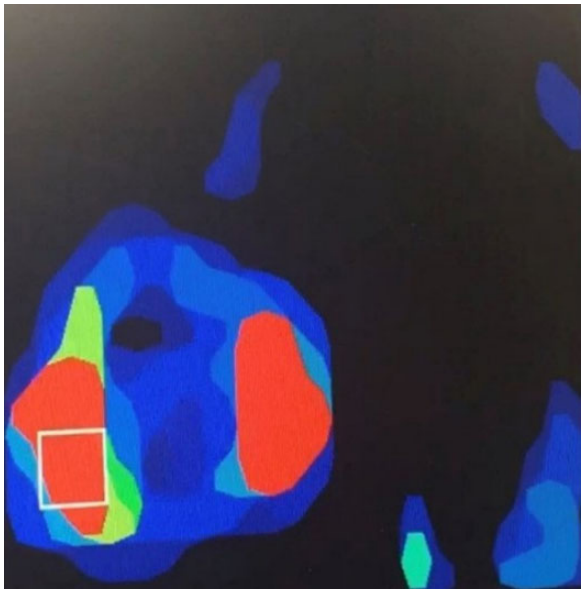

Figure 3. Pressure distribution of a 7.5-mm defect on a lateral femoral condyle.

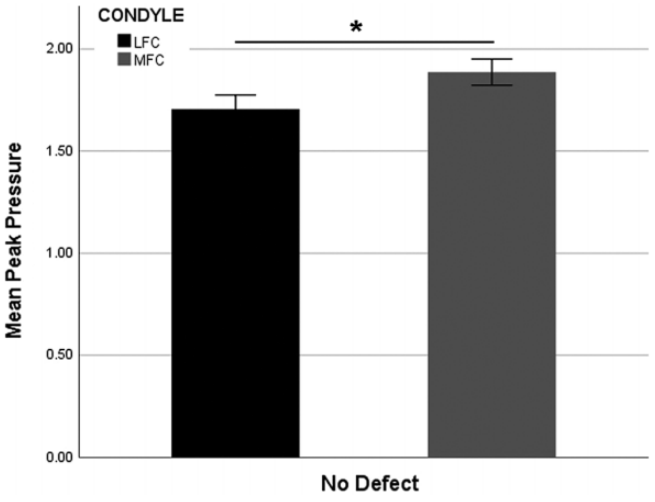

Figure 4. Mean peak pressure at medial femoral condyle (MFC) and lateral femoral condyle (LFC) in goat knees without defect. *$P < .05$. Error bars represent 95% CI.

In the group 3 knees, the peak pressure at the defect rim for the LFC at full extension increased by 139.14% from no defect (1.704 MPa) to a 7.5-mm defect (4.075 MPa) ($P < .001$) and by 117.1% from a 3-mm defect (1.877 MPa) to a 7.5-mm defect (4.075 MPa) ($P < .001$) (Figure 6).

For the isolated 3-mm defects between groups 2 and 3, the peak pressure on the MFC in group 2 (2.279 MPa) was significantly higher vs that on the LFC in group 3 (1.877 MPa) at full extension ($P < .001$) (Figure 7). In contrast, the peak pressures at the defect rim were significantly greater for group 3 vs group 2 at defect diameters of 5 mm ($P < .012$) and 7.5 mm ($P < .0001$).

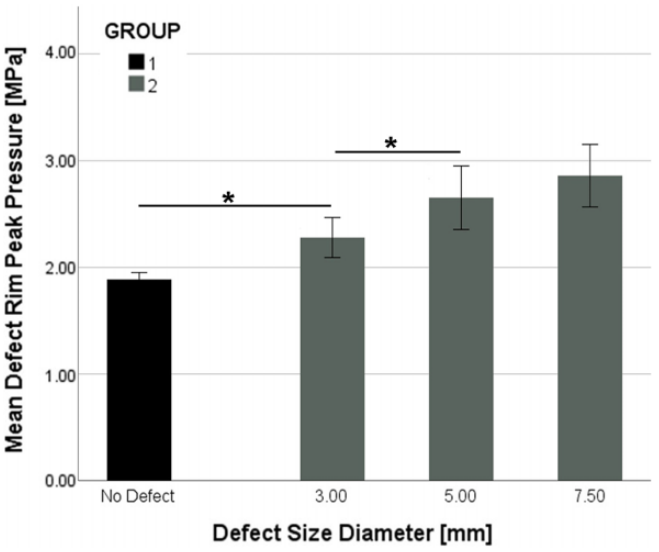

Figure 5. Mean peak pressure at the defect rim for progressively increasing defects at the medial femoral condyle (group 2). *$P < .05$. Error bars represent 95% CI.

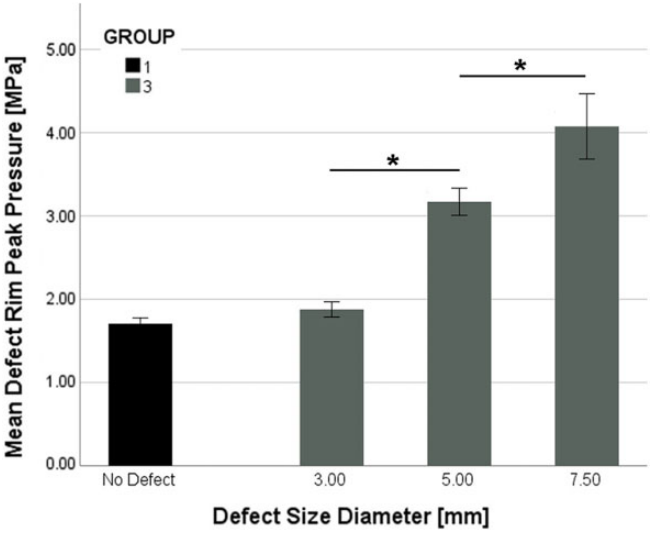

Figure 6. Mean peak pressure at the defect rim for progressively increasing defects at the lateral femoral condyle (group 3). *$P < .05$. Error bars represent 95% CI.

In group 5, for equivalent 3-mm defects on both condyles, the peak pressure for the MFC at full extension was significantly higher than that for the LFC ($P < .001$). However, as the lateral defect diameter was increased to 5 and 7.5 mm, peak pressures for the LFC at full extension were significantly greater than those for the MFC (Figure 8). Moreover, as the lateral defect diameter increased from 3 to 7.5 mm, peak pressures on the constant 3-mm defect of the MFC were significantly different from one another ($P < .001$). The greatest difference in pressure between the LFC and MFC occurred at the 3-mm defect on both condyles. Peak

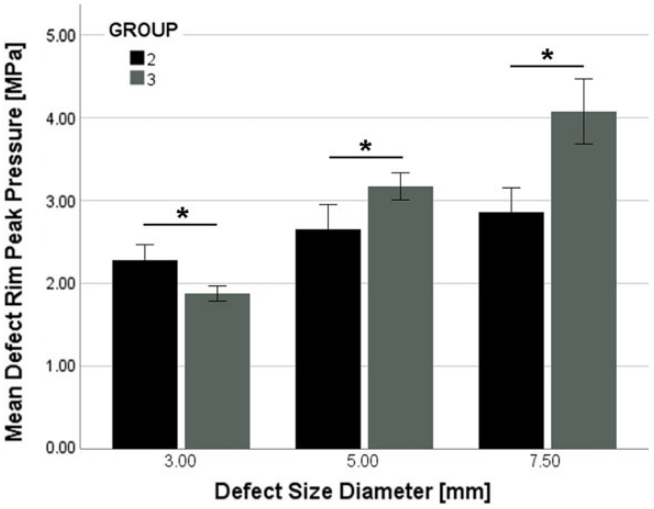

Figure 7. Comparison of mean peak pressure at defect rim for progressively increasing defect size at medial femoral condyle (group 2) vs lateral femoral condyle (group 3). *$P < .05$. Error bars represent 95% CI.

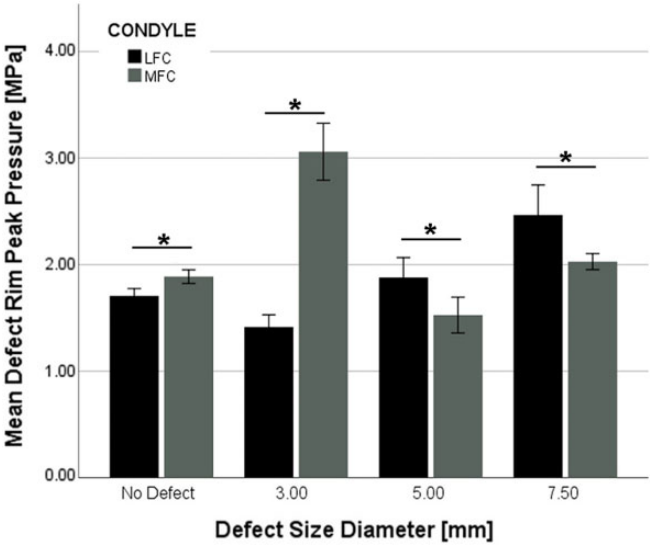

Figure 8. Mean peak pressure at full extension on MFC and LFC for increasing LFC defect size and static 3-mm MFC defect (group 5). *$P < .05$. Error bars represent 95% CI. LFC, lateral femoral condyle; MFC, medial femoral condyle.

pressures on the 3-mm static MFC defect when the LFC defect was 7.50 mm were not significantly different from MFC peak pressures in knees without defect. The peak pressures on the LFC were significantly different from one another across all defect sizes except for the comparison between no defect and a 5-mm defect.

In group 4, for equivalent 3-mm defects on both condyles, mean peak pressure at full extension on the MFC was significantly higher than that on the LFC ($P < .05$). No significant difference in the distribution or mean of defect rim

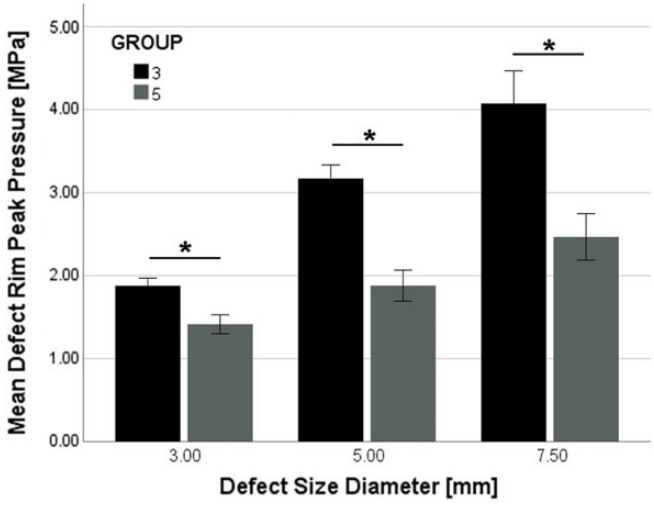

Figure 9. Mean peak pressure at the defect rim at full extension for progressively increasing defect size at the lateral femoral condyle in group 3 (isolated lesion) and group 5 (dual lesion). *$P < .05$. Error bars represent 95% CI.

peak pressures occurred at the MFC for group 4 across the range of other defect diameters, indicating that the static 3-mm defect on the LFC in group 4 altered compartmental loading and pressure distribution differently from the static 3-mm defect on the MFC in group 5.

For the MFC at full extension, the distribution of peak pressures across all defect sizes in group 4 was significantly different when compared with the distribution in group 2 ($P < .04$); however, the peak pressure recorded at each defect size was not significantly different between these groups. Regarding the LFC at full extension, the peak pressures were significantly greater in group 3 vs group 5 at all 3 defect sizes: 32.7% greater at 3 mm (1.877 vs 1.414 MPa; $P < .001$), 68.7% greater at 5 mm (3.170 vs 1.879 MPa; $P < .001$), and 65.2% greater at 7.5 mm (4.075 vs 2.466 MPa; $P < .001$) (Figure 9). No significant difference in mean peak pressure was noted during flexion for equivalent defect sizes between the MFC and LFC. Additionally, no significant difference in mean peak pressure was noted during flexion as the defect size was progressively increased on each condyle.

DISCUSSION

Under dynamic testing through a range of motion, substantial increases in peak pressure were identified at the rim of articular cartilage defects, and these effects increased with the size of the lesions. This suggests a mechanism by which smaller defects can rapidly progress into larger ones. The stress concentration at the defect rim increased to a greater degree for equivalent increases in defect diameter size on the LFC (139.14%) vs the MFC (51.51%) for isolated full-thickness lesions at full extension, and the defect diameter played a significant role independent of location for peak pressures on the MFC and LFC (Figure 7). The increased

defect rim pressure progression seen on the LFC vs MFC may be explained by the biomechanics and condylar geometry of the goat tibiofemoral joint. In the 3-dimensional finite element model of the tibiofemoral joint put forth by Peña et al,[26] the peak contact and shear stress in articular cartilage increased by 200% after a lateral vs medial meniscectomy, and >51% of the total axial load passed through the lateral meniscus vs 30% through the medial meniscus. However, this finding was seen in the human knee, with significantly different biomechanical properties when compared with the unguligrade knee. Additionally, in a bovine model, Flanigan et al[8] noted a lower size threshold for significant subchondral bone contact for LFC defects vs MFC defects, which may help to explain the increased defect rim pressure progression seen in our goat model without menisci.

Compartmental geometry may contribute to this difference: Lateral defects are convex-concave in the frontal plane and convex-convex in the sagittal plane, whereas medial defects have a convex-concave interaction between the femur and tibia in the frontal and sagittal plane. The aforementioned compartmental geometry, with the decrease in contact area from the removal of menisci, may influence the contact of articulating surfaces within and peripheral to the defect.[18] The increased defect rim pressure progression in the lateral compartment may help to explain the relatively higher risk of tibiofemoral articular degeneration and greater tendency for cartilage deterioration seen in patients after a lateral meniscectomy vs a medial meniscectomy.[2,17,26] Additionally, the significantly greater increase in pressure progression on the LFC may partly contribute to the clinical association between lateral defects and subchondral bone overgrowth in patients undergoing autologous chondrocyte implantation and explain why in this subset of patients there has been a longer duration of symptoms attributed to subchondral bone stiffening secondary to microcracks and microfractures.[2,11,14,23,29]

Our findings differed from the biomechanical study in human cadaveric knees with intact menisci by Guettler et al,[13] who noted significantly elevated MFC defect rim peak pressures when compared with LFC defect rim pressures; the authors also found that while mean peak pressures at the defect rim were significantly elevated, they did not significantly differ from one another for progressively increased defect sizes. Notably, testing was performed at a fixed 30° of knee flexion. Similarly, in a canine knee model loaded at 40° of knee flexion, Brown et al[3] found only moderate elevations (10%-30%) in peak contact pressure for articular cartilage defects and no significant effect of increasing defect size. Additionally, our findings diverged from the finite element simulation of the human tibiofemoral joint by Peña et al,[25] who did not find significant differences in compressive and shear stress after meniscectomy for lesions of differing sizes with the knee in simulated full extension. This discrepancy in the results of our biomechanical study can be attributed to several factors. The previous studies were performed at a fixed degree of knee flexion, unlike our evaluation through a dynamic range of motion. Edge loading effects will be accentuated since loading will not be distributed evenly around the rim of the defect. Other factors include differences in articular contact between the goat and human tibiofemoral joint and the removal of menisci from the goat knee. In the goat, the tibial plateau has greater convexity; its menisci cover a larger proportion of the tibial articular surface; and there is a greater similarity in articular congruity between condyles because of its fused fibula.[12,16,22,28]

In our goat model, pressures on the MFC in knees without defect were 10.7% greater at full extension than pressures on the LFC. This percentage increase was lesser in magnitude when compared with the results by Bruns et al[4] in their human cadaveric model, who noted that pressure in the MFC in a neutral position was 26.9% greater than that on the LFC. This difference can be attributed to a decrease in articular congruity between condyles in the goat model because of its fused fibula, convex lateral tibial plateau, and condylar and compartmental joint geometry and from the effects of dynamic loading.[4,22,28]

Our study additionally found that dual lesions may affect compartmental loading but differently depending on which condyle has the increasing defect size. Between isolated LFC defects (group 3) of progressively increasing diameter and dual defects where the LFC defect is progressively increased and the MFC defect remains constant (group 5), the mean peak pressure across all defect sizes was significantly greater for isolated LFC lesions. This finding may result from the compartmental offloading attributed to the convex-concave interaction between the femur and tibia in the frontal and sagittal plane for the MFC defect. Interestingly, no significant difference was seen for the mean peak pressure at the defect rim for progressively increased isolated MFC lesions (group 2) vs dual defects where the MFC defect is progressively increased and the LFC defect remains constant (group 4), potentially indicating that a constant LFC defect did not significantly alter compartmental offloading. Both findings are a by-product of femoral condylar geometry and defect geometry interaction. The process of cartilage degeneration progression has been linked to significant subchondral bone contact and increasing defect diameter.[5,15,20,21,27,29,30,34] Findings from our biomechanical study in a goat model suggest that the location of the defect plays a differential role in pressure transmission. If replicated within a human cadaveric model, this would indicate that lateral compartment chondral lesions are more likely to progress at an earlier stage and that relatively more aggressive cartilage surgical interventions are needed for lateral vs medial lesions in patients with combined meniscal deficiency and ipsilateral chondral disease.

Limitations

There are numerous limitations to our study. The result of removing both menisci for our specimen meant that in vivo loading conditions were not adequately simulated, as femoral cartilage articulates with menisci at the tibial surface and lateral menisci bear a greater proportion of load vs medial menisci. However, the experimental protocol in our

study required removal of both menisci to consistently place a defect in the weightbearing location across each specimen as well as to reliably obtain biomechanical contact parameters around the defect.[19] Additionally, the removal of the long digital extensor and popliteus was a limitation, as with removal, it could alter the weightbearing mechanism under dynamic loading, particularly with regard to the popliteus. Our experimental approach utilized a weighted pulley system to mimic equal contact between the medial and lateral condyles under dynamic flexion and extension. The loading apparatus did not adjust for rotation/translation or varus/valgus movements and was an additional limitation. Given the interspecimen variability, and despite our efforts to mechanically adjust for this, equal distribution was never perfectly achieved. Additionally, the use of goat knees was a limitation, as human cadaveric knees would have been optimal.

CONCLUSION

Increasing defect size resulted in a substantial elevation of peak pressures at the rim of articular cartilage defects when knees were loaded through a range of motion. Isolated LFC defects experienced a greater increase in defect rim stress concentrations when compared with isolated MFC defects for equivalent increases in defect diameters. Defect diameter played a significant role independent of location for peak pressures on the medial and lateral condyles.

REFERENCES

1. Alford JW, Cole BJ. Cartilage restoration, part 2: techniques, outcomes, and future directions. *Am J Sports Med*. 2005;33(3):443-460. doi:10.1177/0363546505274578
2. Alford JW, Lewis P, Kang RW, Cole BJ. Rapid progression of chondral disease in the lateral compartment of the knee following meniscectomy. *Arthroscopy*. 2005;21(12):1505-1509. doi:10.1016/j.arthro.2005.03.036
3. Brown TD, Pope DF, Hale JE, Buckwalter JA, Brand RA. Effects of osteochondral defect size on cartilage contact stress. *J Orthop Res*. 1991;9(4):559-567. doi:10.1002/jor.1100090412
4. Bruns J, Volkmer M, Luessenhop S. Pressure distribution in the knee joint—influence of flexion with and without ligament dissection. *Arch Orthop Trauma Surg*. 1994;113:204-209. doi:10.1007/BF00441833
5. Burr DB, Radin EL. Microfractures and microcracks in subchondral bone: are they relevant to osteoarthrosis? *Rheum Dis Clin North Am*. 2003;29(4):675-685. doi:10.1016/S0889-857X(03)00061-9
6. Davies-Tuck ML, Wluka AE, Wang Y, et al. The natural history of cartilage defects in people with knee osteoarthritis. *Osteoarthritis Cartilage*. 2008;16(3):337-342. doi:10.1016/j.joca.2007.07.005
7. Englund M, Lohmander LS. Risk factors for symptomatic knee osteoarthritis fifteen to twenty-two years after meniscectomy. *Arthritis Rheum*. 2004;50(9):2811-2819. doi:10.1002/art.20489
8. Flanigan DC, Harris JD, Brockmeier PM, Lathrop RL, Siston RA. The effects of defect size, orientation, and location on subchondral bone contact in oval-shaped experimental articular cartilage defects in a bovine knee model. *Knee Surg Sports Traumatol Arthrosc*. 2014;22(1):174-180. doi:10.1007/s00167-012-2342-6
9. Flanigan DC, Harris JD, Brockmeier PM, Siston RA. The effects of lesion size and location on subchondral bone contact in experimental knee articular cartilage defects in a bovine model. *Arthroscopy*. 2010;26(12):1655-1661. doi:10.1016/j.arthro.2010.05.017
10. Gardiner BS, Woodhouse FG, Besier TF, et al. Predicting knee osteoarthritis. *Ann Biomed Eng*. 2016;44(1):222-233. doi:10.1007/s10439-015-1393-5
11. Getgood A, Bhullar TPS, Rushton N. Current concepts in articular cartilage repair. *Orthop Trauma*. 2009;23(3):189-200. doi:10.1016/j.mporth.2009.05.002
12. Griffith CJ, LaPrade RF, Coobs BR, Olson EJ. Anatomy and biomechanics of the posterolateral aspect of the canine knee. *J Orthop Res*. 2007;25(9):1231-1242. doi:10.1002/jor.20422
13. Guettler JH, Demetropoulos CK, Yang KH, Jurist KA. Osteochondral defects in the human knee: influence of defect size on cartilage rim stress and load redistribution to surrounding cartilage. *Am J Sports Med*. 2004;32(6):1451-1458. doi:10.1177/0363546504263234
14. Henderson IJP, La Valette DP. Subchondral bone overgrowth in the presence of full-thickness cartilage defects in the knee. *Knee*. 2005;12(6):435-440. doi:10.1016/j.knee.2005.04.003
15. Hosseini SM, Wilson W, Ito K, Van Donkelaar CC. A numerical model to study mechanically induced initiation and progression of damage in articular cartilage. *Osteoarthritis Cartilage*. 2014;22(1):95-103. doi:10.1016/j.joca.2013.10.010
16. Jackson DW, Lalor PA, Aberman HM, Simon TM. Spontaneous repair of full-thickness defects of articular cartilage in a goat model: a preliminary study. *J Bone Joint Surg Am*. 2001;83(1):53-64. doi:10.2106/00004623-200101000-00008
17. Knapik DM, Harrison RK, Siston RA, Agarwal S, Flanigan DC. Impact of lesion location on the progression of osteoarthritis in a rat knee model. *J Orthop Res*. 2015;33(2):237-245. doi:10.1002/jor.22762
18. Koo S, Andriacchi TP. A comparison of the influence of global functional loads vs local contact anatomy on articular cartilage thickness at the knee. *J Biomech*. 2007;40(13):2961-2966. doi:10.1016/j.jbiomech.2007.02.005
19. Lefkoe TP, Trafton PG, Ehrlich MG, et al. An experimental model of femoral condylar defect leading to osteoarthrosis. *J Orthop Trauma*. 1993;7(5):458-467. doi:10.1097/00005131-199310000-00009
20. Minas T, Gomoll AH, Rosenberger R, Royce RO, Bryant T. Increased failure rate of autologous chondrocyte implantation after previous treatment with marrow stimulation techniques. *Am J Sports Med*. 2009;37(5):902-908. doi:10.1177/0363546508330137
21. Minas T, Nehrer S. Current concepts in the treatment of articular cartilage defects. *Orthopedics*. 1997;20(6):525-538. doi:10.3928/0147-7447-19970601-08
22. Moran CJ, Ramesh A, Brama PAJ, O'Byrne JM, O'Brien FJ, Levingstone TJ. The benefits and limitations of animal models for translational research in cartilage repair. *J Exp Orthop*. 2016;3(1):1-12. doi:10.1186/s40634-015-0037-x
23. Paletta GA, Manning T, Snell E, Parker R, Bergfeld J. The effect of allograft meniscal replacement on intraarticular contact area and pressures in the human knee: a biomechanical study. *Am J Sports Med*. 1997;25(5):692-698. doi:10.1177/036354659702500519
24. Pape D, Filardo G, Kon E, van Dijk CN, Madry H. Disease-specific clinical problems associated with the subchondral bone. *Knee Surg Sports Traumatol Arthrosc*. 2010;18(4):448-462. doi:10.1007/s00167-010-1052 -1
25. Peña E, Calvo B, Martínez MA, Doblaré M. Effect of the size and location of osteochondral defects in degenerative arthritis: a finite element simulation. *Comput Biol Med*. 2007;37(3):376-387. doi:10.1016/j.compbiomed.2006.04.004
26. Peña E, Calvo B, Martinez MA, Palanca D, Doblaré M. Why lateral meniscectomy is more dangerous than medial meniscectomy: a finite element study. *J Orthop Res*. 2006;24(5):1001-1010. doi:10.1002/jor.20037
27. Poulet B, de Souza R, Kent AV, et al. Intermittent applied mechanical loading induces subchondral bone thickening that may be intensified locally by contiguous articular cartilage lesions. *Osteoarthritis Cartilage*. 2015;23(6):940-948. doi:10.1016/j.joca.2015.01.012

28. Proffen BL, McElfresh M, Fleming BC, Murray MM. A comparative anatomical study of the human knee and six animal species. *Knee*. 2012;19(4):493-499. doi:10.1016/j.knee.2011.07.005
29. Radin EL, Rose RM. Role of subchondral bone in the initiation and progression of cartilage damage. *Clin Orthop Relat Res*. 1986;213: 34-40. doi:10.1097/00003086-198612000-00005
30. Saarakkala S, Julkunen P, Kiviranta P, Mäkitalo J, Jurvelin JS, Korhonen RK. Depth-wise progression of osteoarthritis in human articular cartilage: investigation of composition, structure and biomechanics. *Osteoarthritis Cartilage*. 2010;18(1):73-81. doi:10.1016/j.joca.2009.08.003
31. Schinhan M, Gruber M, Vavken P, et al. Critical-size defect induces unicompartmental osteoarthritis in a stable ovine knee. *J Orthop Res*. 2012;30(2):214-220. doi:10.1002/jor.21521
32. Scott CEH, Nutton RW, Biant LC. Lateral compartment osteoarthritis of the knee: biomechanics and surgical management of end-stage disease. *Bone Joint J*. 2013;95B(4):436-444. doi:10.1302/0301-620X.95B4.30536
33. Speirs AD, Beaulé PE, Ferguson SJ, Frei H. Stress distribution and consolidation in cartilage constituents is influenced by cyclic loading and osteoarthritic degeneration. *J Biomech*. 2014;47(10):2348-2353. doi:10.1016/j.jbiomech.2014.04.031
34. Zevenbergen L, Smith CR, Van Rossom S, et al. Cartilage defect location and stiffness predispose the tibiofemoral joint to aberrant loading conditions during stance phase of gait. *PLoS One*. 2018;13(10):e0205842. doi:10.1371/journal.pone.0205842